Biomaterials Science

PAPER

View Article Online
View Journal | View Issue

Cite this: *Biomater. Sci.*, 2016, **4**, 849

Targeted delivery of microRNA-126 to vascular endothelial cells *via* REDV peptide modified PEG-trimethyl chitosan†

Fang Zhou,‡[a] Xiaoling Jia,‡[b] Qingmao Yang,[b] Yang Yang,[a] Yunhui Zhao,[a] Yubo Fan*[b,c] and Xiaoyan Yuan*[a]

Received 23rd December 2015,
Accepted 25th February 2016

DOI: 10.1039/c5bm00629e

www.rsc.org/biomaterialsscience

Manipulation of gene expression by means of microRNAs (miRNAs) is one of the emerging strategies to treat cardiovascular and cancer diseases. Nevertheless, efficient delivery of miRNAs to a specific vascular tissue is limited. In this work, a short peptide Arg-Glu-Asp-Val (REDV) was linked to trimethyl chitosan (TMC) *via* a bifunctional poly(ethylene glycol) (PEG) linker for the targeted delivery of microRNA-126 (miRNA-126) to vascular endothelial cells (VECs). The morphology, serum stability and cytotoxicity of the polyplex/miRNA complexes, namely, TMC/miRNA, TMC-*g*-PEG/miRNA and TMC-*g*-PEG-REDV/miRNA, were investigated along with the cellular uptake, proliferation and *in vitro* miRNA transfection efficiency. By REDV modification, the TMC-*g*-PEG-REDV/miRNA complex showed negligible cytotoxicity, increased expression of miRNA-126 and enhanced VEC proliferation compared with the TMC/miRNA and TMC-*g*-PEG/miRNA complexes. In particular, the approaches adopted for the miRNA delivery and targeted peptide REDV modification promote the selective uptake and the growth of VECs over vascular smooth muscle cells. It was suggested that the REDV peptide-modified TMC-*g*-PEG polyplex could be potentially used as a miRNA carrier in artificial blood vessels for rapid endothelialization.

Introduction

RNA interference presents the therapeutic potential to treat cancer, cardiovascular and other pathologies whose etiology is related to aberrant gene expression.[1–6] MicroRNAs (miRNAs) are endogenously expressed small non-coding RNAs (18–25 nucleotides) that can function as post-transcriptional regulators for gene expression.[1,2] miRNAs have attracted much interest because they are conserved across almost all animal species, thereby emphasizing their evolutionary importance as modulators of critical pathways and processes.[3–6] In the field of vascular biology, miRNA-126 is one of the most important miRNAs that manipulates vascular integrity and angiogenesis *via* regulation of the signaling for angiogenic growth factors.[7–9]

Angiogenic growth factors, such as the vascular endothelial growth factor (VEGF) and fibroblast growth factor (FGF), can modulate adhesion, proliferation and migration of vascular endothelial cells (VECs) by activating the MAP kinase pathway, which culminates in the nucleus to enhance the expression of genes required for angiogenesis and vascular integrity.[7] It was reported that miRNA-126 regulated the response of VECs to angiogenic growth factors.[7,8] In the absence of miRNA-126, increased expression of SPRED1 and PIK3R2 diminishes the transmission of intracellular angiogenic signals by VEGF and FGF.[8] Therefore, investigation of the miRNA-126 function allowed us to know that miRNA-126 can be used as a VEC-specific regulator of angiogenic signaling.

VECs initially differentiate from angioblastic precursors and then proliferate and migrate to form the primitive vascular plexus through the process of vasculogenesis.[8] VECs play essential roles in the maintenance of vascular integrity, angiogenesis, and wound repair. Previous studies have demonstrated that the injury-induced migration of VECs and the delayed re-endothelialization as well as the proliferation of vascular smooth muscle cells (VSMCs) are the major pathophysiological events that lead to neointima formation.[10–13] And, the vessel endothelium is of vital importance in maintaining the vessel integrity by inhibiting thrombosis and hyperplasia. Many studies focused on improving the rapid endothelialization by means of bioactive molecules immobilization,[10–12] and it was also noted that VECs would be rivals of other cell types *in vivo*.[14] Therefore, it is necessary to make efforts to specifi-

[a]*School of Materials Science and Engineering, and Tianjin Key Laboratory of Composite and Functional Materials, Tianjin University, Tianjin 300072, China. E-mail: yuanxy@tju.edu.cn, xyuan28@yahoo.com*
[b]*Key Laboratory for Biomechanics and Mechanobiology of Ministry of Education, School of Biological Science and Medical Engineering, Beihang University, Beijing 100083, China. E-mail: yubofan@buaa.edu.cn*
[c]*National Research Center for Rehabilitation Technical Aids, Beijing 100176, China*
†Electronic supplementary information (ESI) available. See DOI: 10.1039/c5bm00629e
‡These authors contributed equally to this work.

cally enhance VEC growth considering the cell competition. Ji's group has demonstrated that the competitive growth of human umbilical vein endothelial cells over human aortic smooth muscle cells could be increased *via* the specific recognition of the short peptide Arg-Glu-Asp-Val (REDV) on the cardiovascular stent.[14] The REDV peptide is a VEC-specific ligand that mediates the adhesion and migration of VECs *via* the integrin α4β1 subunit, instead of allowing the adhesion of VSMCs and platelets.[15,16]

It is hypothesized that RNA interference and specific peptide-mediated therapies are effective strategies to promote endothelialization.[17] Then, it is essential to develop an ideal system for the delivery of miRNA that confers physical stability to the unstable RNA structure, protects the RNA from nuclease degradation and aids in effective silencing of target genes. As principal nonviral vehicles, cationic polymers have been widely investigated in recent years.[4] Trimethyl chitosan (TMC) has been developed *in vitro* and *in vivo* for the delivery of RNA and DNA because of its cationic charge, biodegradability and biocompatibility, as well as the permeability-enhancing properties.[18–20] And, it was reported that the pH dependency of the chitosan complexation has been significantly reduced with high efficiency in inducing gene silencing.[19]

Poly(ethylene glycol) (PEG) could strongly decrease cytotoxic effects and further increase the solubility and colloidal stability of TMC, resulting in an increased polyplex uptake of the complexation.[21–25] The modified delivery vehicles by a peptide derived from the rabies virus glycoprotein *via* a PEG linker not only increase the spatial freedom of the peptide molecules and efficient binding but also help increase the biocompatibility, serum stability, and systemic circulation time of the complexes.[23] Zhang *et al.* also found that PEG conjugated *N*-(2-hydroxy)propyl-3-trimethyl ammonium chitosan chloride with 9% PEGylation degree had good transfection efficiency about 5.3-fold higher than a quaternized chitosan.[25]

For actual application, it is very important to construct active RNA carriers which can be taken up specifically by VECs to enhance endothelialization. Feng's group has made attempts.[17,26] In this work, the targeting REDV peptide-modified TMC was prepared through a bifunctional PEG for the targeted delivery of miRNA-126 to VECs. Three polyplexes, *i.e.*, TMC, TMC-*g*-PEG and TMC-*g*-PEG-REDV were condensed with miRNA-126 to generate polyplex/miRNA-126 complexes. The complexes were systematically characterized, and the VEC-targeting ability, cellular proliferation and miRNA transfection efficiency were evaluated. It was hypothesized that the prepared cationic complexes self-assembled from TMC-*g*-PEG-REDV could target delivery of miRNA-126 to VECs owing to the active target REDV ligands on the surface.

Experimental methods

Materials

Chitosan (molecular weight ~50 kDa, deacetylation degree 95%) was purchased from Haidebei Marine Bioengineering Co., Ltd (Jinan, China). Methoxy-poly(ethylene glycol)-succinimidyl carboxy methyl ester (mPEG-SCM, 5 kDa) and ω-2-pyridyldithio polyethylene glycol α-succinimidylester (OPSS-PEG-SCM, 5 kDa) were purchased from Jenkem Technology Co., Ltd, China. Methyl iodide was obtained by Xiya reagent, China. The REDV-Cys peptide sequence (Arg-Glu-Asp-Val-Cys) was purchased from Shanghai Science Peptide Biological Technology Co., Ltd, China. miRNA-126 mimics (sense 5′-UCG UAC CGU GAG UAA UAA UGC G-3′, antisense 5′-CAU UAU UAC UCA CGG UAC GAU U-3′), negative control miRNA, carboxyfluorescein-labeled miRNA (FAM-miRNA), RNA purification kit and hairpin-it™ miRNAs qPCR quantitation kit were supplied by Gene Pharma Co., Ltd, China. Fetal bovine serum (FBS), M199 and DMEM were supplied by Gibco, USA. Cell counting kit-8 (CCK-8) was purchased from Dojindo, Japan. Heparin sodium salt (159 units per mg) was obtained from Shanghai Chemical Reagent, China. Phosphate buffer saline (PBS) solution (pH 7.4, 0.1 M), Tris-acetate-EDTA (TAE) buffer and *N*-methyl-2-pyrrolidone were as provided by Tianjin Runtai Technology Ltd, China.

Synthesis of TMC

TMC was synthesized by reductive methylation of chitosan with methyl iodide according to the literature.[27] In brief, chitosan (1 g) and sodium iodide (2.4 g) were added to a mixture of 15% (w/v) aqueous NaOH solution (5.6 mL) and *N*-methyl-2-pyrrolidone (40 mL). The mixture was then heated to 60 °C. Methyl iodide (6 mL) was added, and the mixture was refluxed for 45 min. Then, additional methyl iodide (3 mL) and 15% (w/v) aqueous NaOH solution (5.6 mL) were added to the mixture while stirring was continued for another 45 min at 60 °C. The product was precipitated with ethanol and isolated by centrifugation. After washing with diethyl ether, the final product was dissolved in 10% (w/v) aqueous NaCl solution (40 mL) and stirred for 3 h for ion-exchange. The obtained solution was dialyzed (MWCO 10 kDa) against deionized water and then lyophilized to obtain TMC.

Synthesis of TMC-*g*-PEG and TMC-*g*-PEG-REDV

TMC (10 mg) was reacted with a bifunctional PEG (ω-2-pyridyldithio polyethylene glycol α-succinimidylester, OPSS-PEG-SCM) (30 mg) in distilled water for 6 h at room temperature, allowing the primary amino groups on TMC to react specifically with the SCM group of the heterobifunctional PEG (Fig. 1). The obtained solution was dialyzed (MWCO 10 kDa) against deionized water and then lyophilized to obtain TMC-*g*-PEG-OPSS. Then, the obtained TMC-*g*-PEG-OPSS reacted with REDV-Cys in distilled water for 2 h at room temperature to link the REDV peptide by means of a specific reaction between the OPSS group in TMC-*g*-PEG-OPSS and the thiol group in the REDV-Cys peptide. The TMC-*g*-PEG polyplex was prepared in the same way except that the bifunctional PEG (OPSS-PEG-SCM) was replaced by mPEG-SCM.

^{1}H nuclear magnetic resonance (^{1}H NMR)

^{1}H NMR spectra of the polymers were recorded on a Varian spectrometer (INOVA 500 MHz and Infinity plus 300WB, USA)

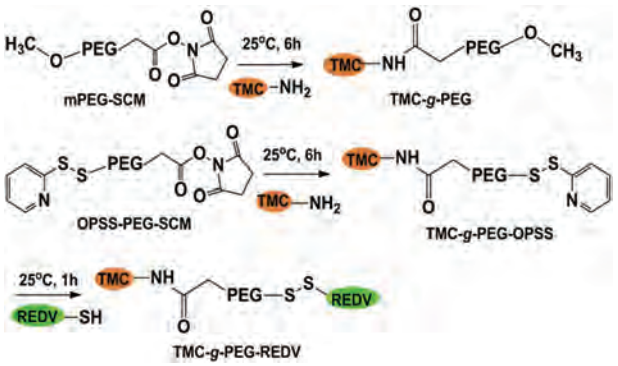

Fig. 1 Synthesis of TMC-*g*-PEG and TMC-*g*-PEG-REDV.

in D_2O as the solvent at room temperature. The degree of quaternization (DQ) of TMC was calculated using eqn (1) as described in ref. 27.

$$\mathrm{DQ}\,(\%) = \frac{[(\mathrm{CH_3})_3]}{9[\mathrm{H}]} \times 100 \quad (1)$$

where, $[(CH_3)_3]$ is the integral of the trimethyl amino group peak at 3.3 ppm, and [H] is the integral of the ^{1}H peaks from 4.7 to 5.7 ppm from ^{1}H NMR.

The number of PEG chains as a percentage of the total nitrogen number per TMC-*g*-PEG molecule (graft ratio, GR) was calculated using eqn (2):

$$\mathrm{GR}\,(\%) = \frac{[\mathrm{PEG}]}{438[\mathrm{H}]} \times 100 \quad (2)$$

where, [PEG] is the integral of the proton peak of the PEG block at 3.65 ppm ($-OCH_2-$). The number of protons per PEG chain is 438 according to the molecular mass of mPEG-SCM given by the supplier. [H] is the integral intensity from 4.7 to 5.7 ppm in ^{1}H NMR.

Preparation of polyplex/miRNA complexes

The polyplex/miRNA complexes were formed by the electrostatic interaction of the cationic polymer TMC, TMC-*g*-PEG and TMC-*g*-PEG-REDV (abbreviated as T, TP and TPR) with negatively charged miRNA at a suitable N/P molar ratio. The polyplex/miRNA complexes at various N/P molar ratios were formulated by adding the polyplexes (10 mg mL^{-1}) to a certain volume of a defined miRNA solution. Then the mixtures were incubated at room temperature for 30 min to allow complex formation completely. TMC/miRNA, TMC-*g*-PEG/miRNA and TMC-*g*-PEG-REDV/miRNA complexes were designated as T–miRNA, TP–miRNA and TPR–miRNA, respectively.

Gel retardation assay

The polyplex/miRNA complexes at different N/P molar ratios were prepared freshly as described above. The complex solution (9 μL) was mixed with a miRNA loaded buffer, and added into 2% agarose gel containing ethidium bromide (0.5 mg mL^{-1}). The electrophoresis experiment was performed for 20 min in 1× TAE buffer at 100 V, and the image was captured through BioImaging Systems (UVP, LLC, Germany).

Size and zeta potential measurements

The sizes and zeta potentials of polyplex/miRNA complexes were measured by dynamic light scattering (DLS) using a Zetasizer Nano ZS 90 (Malvern Instruments, Ltd, UK). Complex solutions containing 5 μg mL^{-1} miRNA were prepared at N/P ratios of 6, 12, 24 and 48. The size (by intensity, *z*-average radii) and zeta potentials were presented as the mean values of three measurements ± SD (standard deviation).

Transmission electron microscopy (TEM)

The polyplex/miRNA complexes at N/P = 12 were viewed under a JEM-100CX II transmission electron microscope (Jeol, Japan) after negatively stained with 1.5 wt% phosphotungstic acid.

Atomic force microscopy (AFM)

The morphology of polyplex/miRNA complexes at N/P = 12 was investigated by AFM (CSPM5500A, Being Nano-Instruments, Ltd, China) in a tapping mode, with samples prepared by spin-coating sample solutions onto freshly cleaved silicon wafers at 1000 rpm. The samples were imaged at 3 μm × 3 μm magnification using a nanosensor silicon tip.

miRNA serum stability

The serum stability of miRNA in TPR was characterized by gel electrophoresis. Naked miRNA and TPR–miRNA (TMC-*g*-PEG-REDV/miRNA) were incubated in PBS containing 50% FBS at 37 °C. At each predetermined time point (0, 6, 12, 24, 48, and 72 h), 30 μL of each sample was collected and stored at −20 °C until gel electrophoresis was performed. To displace miRNA from TPR, 2 μL of heparin (500 U mL^{-1}) was added to each sample and then the integrity of the miRNA was examined by gel electrophoresis.[31]

Cytotoxicity

All experiments were conducted in compliance with Provisions and General Recommendation of Chinese Experimental Animals Administration Legislation, and were approved by Beijing Municipal Science & Technology Commission.

Human umbilical vein endothelial cells (HUVECs, primary culture) were treated with polyplex/miRNA complexes (N/P = 12) at concentrations ranging from 25 μg mL^{-1} to 200 μg mL^{-1} in 96-well plates and cultured in M199 or DMEM in the presence of 10% FBS under a 5% CO_2 atmosphere and at 37 °C. The 500 mL medium was refreshed every 2 days. The proliferation values were examined by the MTT assay (n = 5). The IC_{50} values, which represented the concentration of the complexes resulting in 50% inhibition of cell growth, were also calculated.

Cellular uptake of miRNA loaded complexes

To determine the cellular uptake and specificity of miRNA delivery, VECs and VSMCs (primary culture from Sprague-Dawley rat aorta, passage 3–5) were seeded in 48-well plates at a density of 1 × 10^4 cells per well and incubated overnight.

T–miRNA, TP–miRNA and TPR–miRNA were complexed with FAM-miRNA and mixed in the cell culture medium at final miRNA concentrations of 240 nM. The cells were incubated with the samples for 4 h before being washed twice with PBS and subsequently incubated in complete culture medium for 16 h. The mean fluorescence intensity (MFI) was analyzed by flow cytometry (FCM) using a FACS flow cytometer (BD FACSCalibur).[23]

The cellular uptake of TPR–miRNA was further investigated by confocal laser scanning microscopy (CLSM, Leica TCS SPE). VECs were seeded on glass coverslips in 6-well plates and incubated overnight. Then, the cells were treated with TPR–miRNA at a miRNA concentration of 240 nM (approximately equal to 50 μg mL^{-1} of TPR–miRNA complexes in cell viability test) and then incubated for 4 h. Subsequently, the cells were washed three times with PBS, fixed using 4% paraformaldehyde in PBS and stained with 4′6-diamidino-2-phenylindole (DAPI). Fluorescence images were acquired using CLSM. For DAPI imaging, the employed excitation wavelength was 405 nm and the emission wavelength was 461 nm. For FAM-miRNA imaging, the employed excitation wavelength was 488 nm and the emission wavelength was 520 nm.

Transfection and cell proliferation assays

To measure the miRNA transfection efficiency, VECs were seeded in 48-well plates at a density of 1×10^4 cells per well and incubated overnight. T–miRNA, TP–miRNA and TPR–miRNA were complexed with miRNA-126, respectively and added in the cell culture medium at a final miRNA concentration of 120 nM. The 500 mL medium was refreshed every 2 days. Transfection efficiencies of miRNA-126 were quantified after 3, 6 and 9 days by qRT-PCR (Bio-Rad iQ5, USA) using the RNA purification kit and the hairpin-it™ miRNAs qPCR quantitation kit. The proliferation values were examined by the CCK-8 assay after cell culture for 3, 6 and 9 days, respectively.[28]

Statistical analysis

The data were represented as mean ± SD for at least three separate measurements and compared by using one-way ANOVA tests. A *P*-value less than 0.05 was considered as statistically significant differences between the pairs.

Results and discussion

Characterization of the polyplexes

To improve miRNA transfection efficiency and cell competition, a targeting peptide REDV is introduced in the miRNA delivery system. To improve the solubility and the miRNA complexing ability of chitosan, TMC, TMC-*g*-PEG and TMC-*g*-PEG-REDV were prepared. The quaternization degree of TMCs plays an important role in opening the tight junctions, and a higher degree of substitution would enhance permeation.[20,21] Therefore, TMCs with a substitution degree of 38.0% were prepared, and Fig. 2 illustrates the ^{1}H NMR spectra of TMC, TMC-*g*-PEG, TMC-*g*-PEG-OPSS and TMC-*g*-PEG-REDV, respectively. TMC showed signals at 2.5 ($-N(CH_3)_2$) and 3.3 ($-N^+(CH_3)_3$)

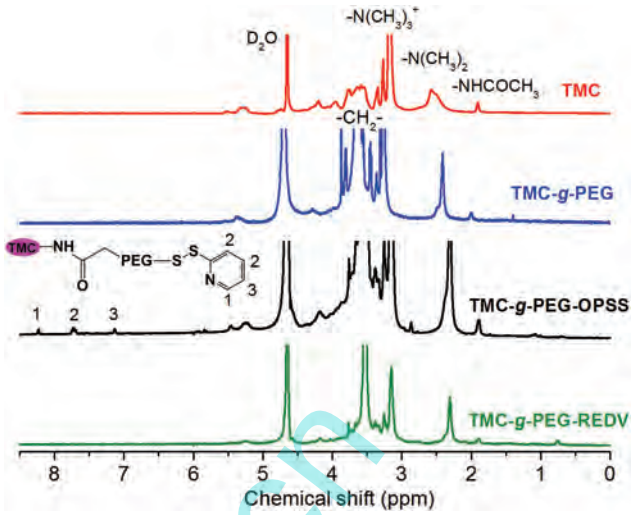

Fig. 2 ^{1}H NMR spectra of TMC, TMC-*g*-PEG, TMC-*g*-PEG-OPSS and TMC-*g*-PEG-REDV in D_2O.

ppm. A signal at 3.8 ppm for PEG ($-CH_2-O-$) also appeared for TMC-*g*-PEG, TMC-*g*-PEG-OPSS and TMC-*g*-PEG-REDV. The estimated graft ratio of PEG was about 18.8% according to the ^{1}H NMR spectra. The cysteine residue at the end of the REDV peptide was used to specifically react with the OPSS groups of TMC-*g*-PEG-OPSS to obtain TMC-*g*-PEG-REDV.[29]

As shown in Fig. 2, a characteristic signal of the OPSS group at 7.1–8.3 ppm appeared for TMC-*g*-PEG-OPSS. Furthermore, the signal of the OPSS group disappeared completely in the ^{1}H NMR spectrum of TMC-*g*-PEG-REDV, suggesting that all the OPSS groups had almost reacted with the thiol groups in the REDV-Cys peptide. The polyplex/miRNA complexes at varied N/P molar ratios were formulated by the electrostatic interaction. The results of characterization of polyplex/miRNA complexes are collected in Table 1.

Gel retardation assay

The condensation ability of miRNA by polyplexes is an important prerequisite for efficient RNA delivery. In the gel retardation assay, T, TP and TPR polyplexes could effectively compact miRNAs, respectively, into relatively stable complexes at N/P molar ratios equal to or greater than 6, 12 and 12 (ESI, Fig. S1†). Polyplex/miRNA complexes were formed by the electrostatic interaction between the cationic polymer and

Table 1 Characterization of polyplex/miRNA complexes

			Modified chitosan	
Sample	N/P ratio	$V_{polyplex}/V_{RNA}$	DQ[a] (%)	GR[b] (%)
T–miRNA	12	3/7	38.0	0
TP–miRNA	12	8/9	38.0	18.8
TPR–miRNA	12	1/1	38.0	18.8

[a] The degree of quaternization of TMC, determined by ^{1}H NMR. [b] The grafting ratio of PEG on TMC, determined by ^{1}H NMR.

negatively charged miRNA. The difference in the binding capacity of polyplexes might result from the linkage of PEG. The linked PEG might produce some steric hindrance and electrostatic shielding or even be buried into the formed complexes.[23] In order to ensure the stability of polyplex/miRNA complexes, the N/P molar ratio of 12 was selected preferentially in the following study.

Size and zeta potential of the polyplex/miRNA complexes

The size and zeta potential of the polyplex/miRNA complexes with N/P molar ratios ranging from 6 to 48 were analyzed by DLS and are given in Table 2. As shown in Table 2, the average size of T–miRNA decreased with the reduction of the N/P molar ratio, and size distributions from 342.1 ± 8.0 nm to 163.0 ± 5.0 nm were observed. However, the average size of TP–miRNA decreased as the N/P molar ratio increased. The size distributions from 157.8 ± 9.0 nm to 103.9 ± 1.7 nm were detected. The sizes of TPR–miRNA complexes were similar to those of the TP–miRNA complexes. The reason could be the steric repulsion effect and the hydration of the hydrophilic PEG chains on the surface, which improved the stability of the complexes. The sizes of the TP–miRNA and TPR–miRNA complexes decreased with the increase of N/P molar ratios because at higher N/P molar ratios the net electrostatic repulsive force could prevent complex aggregation and further stabilize nanoparticles.[25,30] The increasing size of T–miRNA with the rising N/P molar ratio might be partly due to the very high number of positive charges on the complexes. More specifically, at a higher N/P molar ratio, more positively charged molecules of the excess TMC polyplex that did not bind miRNA could aggregate and stretchout due to electrostatic repulsion, resulting in a larger hydrodynamic size. This also corresponded to the result that the zeta potential decreased with the decreasing N/P molar ratio. Similar results were reported by Gao[23] and Katas.[31] The zeta potential of the complexes increased with the N/P molar ratio (Table 2). Besides, the zeta potentials of TP–miRNA and TPR–miRNA were lower than those of T–miRNA complexes, which could be attributed to the stronger shielding effect of PEG chains on the surface of the complexes.[25,32]

Morphology of the polyplex/miRNA complexes

An appropriate morphology and size of polyplex/miRNA complexes are crucial for efficient cell uptake and gene transfection. The morphology of T–miRNA, TP–miRNA and TPR–miRNA complexes was observed by TEM. As shown in TEM micrographs (Fig. 3), the polyplex/miRNA nanoparticles exhibited compact spherical shapes with narrow distribution. The average diameters of the T–miRNA, TP–miRNA and TPR–miRNA complexes were about 79 ± 5.6 nm, 52 ± 2.9 nm and 53 ± 3.2 nm, respectively. TPR–miRNA had a smaller diameter than T–miRNA, consistent with the relative size measured by DLS as shown in Table 2. In AFM topography images, the diameters of the complexes were about 94 ± 6.6 nm, 54 ± 2.7 nm and 55 ± 2.5 nm, respectively (ESI, Fig. S2†). Notably, the sizes of TP–miRNA and TPR–miRNA determined by TEM and AFM were smaller than that observed from the DLS measurements. The size of the complex nanoparticles obtained from the DLS measurements reflected the hydrodynamic size, whereas the results observed by TEM and AFM showed the size of the dried state.[23] Therefore, reduced sizes were observed by TEM and AFM since the hydration shell of the complexes had been removed.

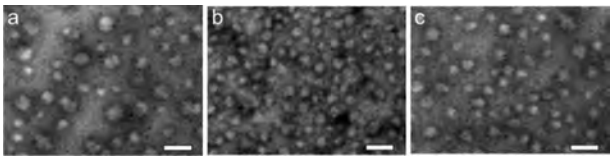

Fig. 3 TEM micrographs of T–miRNA (a), TP–miRNA (b), and TPR–miRNA (c) complexes at N/P = 12. Bars represent 100 nm.

Serum stability

The miRNA protection effect of the TPR polyplex was monitored by 50% serum stability assay with intact miRNA as a positive control. The degradation of the miRNA recovered from TPR–miRNA complexes started after 24 h but complete degradation was not observed even after 72 h (ESI, Fig. S3†). These electrophoretic results revealed that the TPR complex could effectively protect miRNA from degradation by serum in order to transfect miRNA inside the cells.

Cytotoxicity

Quaternization of chitosan improved both the solubility and miRNA-binding efficiency, however, it also brought about cytotoxicity.[19,22] As low toxicity is an essential function for the gene delivery system, the cytotoxicity of the complexes with miRNA was investigated by the MTT assay after 24 h of incubation. As shown in Fig. 4, the cell viability was seen to decrease with the increase of concentrations of all samples. The complexes of TPR–miRNA and TP–miRNA revealed higher

Table 2 Size and zeta potential of the complexes at different N/P molar ratios

	Particle size (nm)			Zeta potential (mV)		
N/P ratio	T–miRNA	TP-miRNA	TPR–miRNA	T–miRNA	TP–miRNA	TPR–miRNA
6	163.0 ± 5.0	157.8 ± 9.0	180.7 ± 11.2	0.5 ± 0.1	0.2 ± 0.2	0.3 ± 0.5
12	174.3 ± 2.0	98.6 ± 2.1	130.2 ± 6.9	8.0 ± 0.3	6.5 ± 0.6	7.0 ± 0.6
24	190.4 ± 3.0	125.6 ± 2.0	110.0 ± 7.6	23.0 ± 1.0	20.0 ± 2.0	20.5 ± 2.0
48	342.1 ± 8.0	103.9 ± 1.7	114.9 ± 1.8	34.0 ± 0.6	27.0 ± 2.1	28.0 ± 3.1

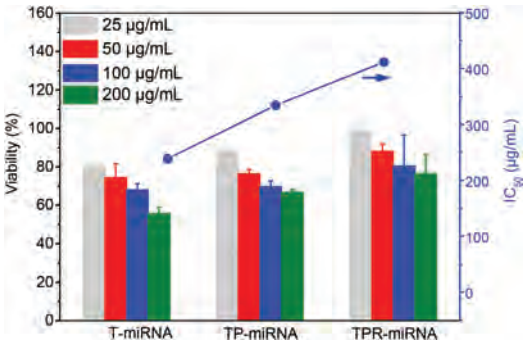

Fig. 4 Cell viability and IC_{50} values of T–miRNA, TP–miRNA and TPR–miRNA measured by the MTT assay. Cell viability is expressed as mean ± SD (n = 3).

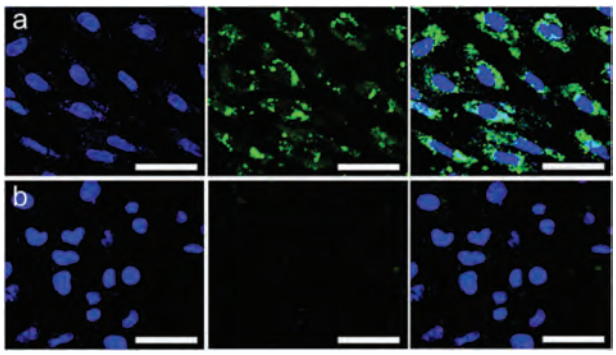

Fig. 5 CLSM images of VECs and VSMCs after treatment with TPR–miRNA for 24 h. For each panel, the images from left to right show cell nuclei stained by DAPI (blue), miRNA fluorescence in cells (green), and overlays of the two images. Bars represent 50 μm. (a) VECs, (b) VSMCs.

cell viabilities than T–miRNA at the same concentration. PEGylation of the TMC could contribute to the decrease of toxicity of the vehicles. The PEG linker was shown to significantly decrease cytotoxic effects and further increase the solubility and colloidal stability of TMC due to the steric repulsion effect and the hydration of PEG chains. The introduced PEG chains enhanced biocompatibility which was also reported by Mao *et al.*[21] After a 24 h incubation, TPR exhibited a high IC_{50} value of 411 μg mL^{-1} and high cell viabilities from which it could be confirmed that TPR–miRNA had negligible toxicity and TPR could be used as a suitable miRNA delivery carrier.

Cellular uptake

Although many studies have focused on improving the rapid endothelialization through the immobilization of bioactive molecules,[10–12] it should be noted that the VECs will compete with VSMCs *in vivo*. The REDV peptide is a VEC-specific ligand that mediates adsorption and migration of VECs *via* the integrin α4β1 subunit.[16] It is expected to increase the VEC uptake of the complexes by using REDV as a target-specific ligand. To confirm the cellular uptake of TPR–miRNA in VECs and VSMCs, CLSM analysis was performed. As shown in Fig. 5a, the strong green fluorescence produced by FAM-miRNA was detected diffused inside the VECs, indicating that much of the TPR–miRNA was internalized and the distribution of TPR–miRNA was quite even in the cell cytoplasm. In contrast, trivial green fluorescence was observed in VSMCs (Fig. 5b). The TPR–miRNA complex could increase the recognition of VECs owing to the specific selectivity between the REDV peptide and the α4β1 integrin of VECs.

The cellular uptake of T–miRNA, TP–miRNA and TPR–miRNA prepared with FAM-miRNA was verified using FCM in VECs and VSMCs, respectively. Quantification was performed by measuring the MFI value. Fig. 6 shows that the MFI values of TPR–miRNA in VECs increased 1.9-fold and 7.5-fold, respectively, higher than the results of T–miRNA and TP–miRNA, at 240 nM. Furthermore, the MFI value of TPR–miRNA in VECs was significantly higher than that of TPR–miRNA in VSMCs. However, no obvious differences between VECs and VSMCs were observed for T–miRNA. And, the MFI value of TP–miRNA in VECs was even lower than that in VSMCs. These

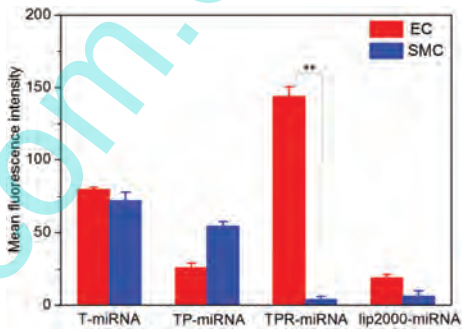

Fig. 6 Cellular uptake of the miRNA complexes and lip2000-miRNA. The mean fluorescence intensity (MFI) was analyzed by FCM. Data are expressed as mean ± SD (n = 3). $^{**}p < 0.01$.

results demonstrated that the REDV peptide decoration on the surface of the complexes could specifically increase the binding affinity, and thus, significantly increase the cellular uptake of TPR–miRNA complexes inside VECs. REDV peptide linking to the TP polyplex could be attributed to the decrease of the non-specific protein adsorption in the FCM test, so that the MFI value of TPR–miRNA in VSMCs was relatively lower than that of TP–miRNA or T–miRNA in VSMCs.

The TPR–miRNA complexes were efficiently and selectively adsorbed onto the surface of the VECs, which facilitated endocytosis, the entrance of complexes into cells. After escaping from the endo/lysosome, the complexes and miRNA could separate out in the cytoplasm. This RNA interference process has been confirmed by Singh and coworkers.[33] The combination of the REDV peptide selectivity and the miRNA delivery could contribute to the competitive adhesion and the growth of VECs over VSMCs.

Transfection and cell proliferation

The transfection efficiency was quantified by the qRT-PCR test. As shown in Fig. 7, with the extension of time, the expression of miRNA-126 in VECs gradually increased. The TPR–miRNA

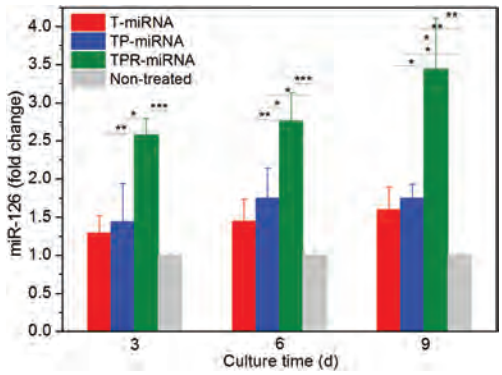

Fig. 7 miRNA-126 expression of VECs treated with different complexes. Data are expressed as mean ± SD (n = 3). *p < 0.05, **p < 0.01, ***p < 0.001.

delivery of miRNA complexes significantly increased the miRNA-126 expression compared with the results of T–miRNA and TP–miRNA. At day 9, miRNA expression efficiencies of ~1.6, 1.7 and 3.4 were detected for T–miRNA, TP–miRNA and TPR–miRNA complexes, respectively, and the results were more significant compared with the non-treated controls, lip2000-miRNA. At each time point, the miRNA expression efficiencies demonstrated a similar tendency, *i.e.*, TPR–miRNA was significantly higher than TP–miRNA and T–miRNA (p < 0.05). As described in the FCM test, REDV peptide decoration on the complexes specifically increased the cellular uptake of TPR–miRNA into the VECs, and thus, increased miRNA expression efficiencies of the TPR–miRNA sample was observed. This observation further confirmed that the combination of the miRNA delivery polyplex and the targeting peptide could promote miRNA-126 transfection in VECs. The result of cell proliferation was similar, as demonstrated in the CCK8 test (Fig. 8).

The miRNA-126 transfer abilities and the cell proliferation values of T–miRNA, TP–miRNA and TPR–miRNA were investigated *in vitro* by the CCK8 test. VECs were seeded with T–miRNA, TP–miRNA and TPR–miRNA complexes, respectively. Their viability and proliferation were evaluated at day 3, 6, and 9. As shown in Fig. 8, the viability values increased with the culture time and showed that the proliferation occurred. At day 3, the values of the TPR–miRNA samples were significantly higher than those of T–miRNA and TP–miRNA. And this phenomenon could also be seen at day 6 and 9 as well. The result demonstrated that miRNA-126 evidently promoted VEC proliferation, which coincided with early research studies that miRNA-126 could promote VEC spread and stimulate the proliferation of VECs.[7,8] Furthermore, compared with T–miRNA and TP–miRNA complexes, TPR–miRNA could be taken up specifically by the VECs. And the targeting TPR–miRNA complexes could enhance the selectivity of VECs over VSMCs, thus promoting the proliferation of VECs. Therefore, these active target TMC-*g*-PEG-REDV polyplexes might be used as efficient miRNA carriers for proliferation of VECs, and these showed great potential to expedite rapid endothelialization in vascular tissue engineering.

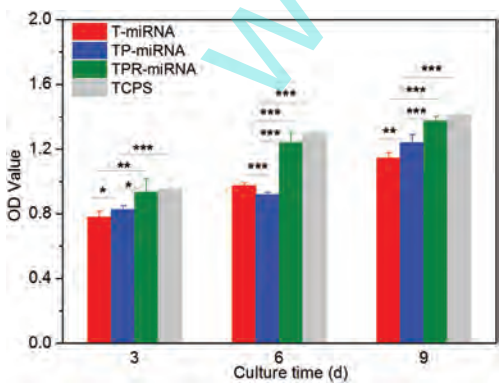

Fig. 8 Cell proliferation of the transfected VECs. Data are expressed as mean ± SD (n = 3). *p < 0.05, **p < 0.01, ***p < 0.001.

Currently, miRNA-based therapeutics are administrated systemically *in vitro* and *in vivo* to stimulate tissue generation.[23,24,34] However, a systemic administration of large doses of miRNA-based therapeutics carries a risk of off-target and undesired effects, because miRNAs can target multiple messenger RNAs in an array of tissue types. It is probably difficult to restrict the cell types and/or tissues exposed to a systemically administered therapeutic miRNA.[35] Thus, it could be assumed that localized miRNA delivery systems would hold significant advantages for localized vascular tissue regeneration. The electrospun nanofibrous scaffolds as vehicles for the localized delivery of TMC-*g*-PEG-REDV/miRNAs complexes will be reported in further work.

Conclusions

The TMC-*g*-PEG-REDV polyplex was developed containing REDV for targeted delivery of miRNAs to VECs. The TMC related polyplexes have the ability of effective compaction of miRNAs. PEGylation of TMC increased the serum stability and decreased the cell toxicity of the polyplexes. The TMC-*g*-PEG-REDV/miRNA-126 complexes exhibited not only favourable physicochemical properties, including increased serum stability and negligible toxicity, but also efficient endothelial cellular uptake, high miRNA transfection efficiency and significantly promoted VEC proliferation. Moreover, the combination of the miRNA delivery polyplex and the targeting peptide REDV could improve the selective uptake and the growth of VECs over VSMCs. It was suggested that the TMC-*g*-PEG-REDV polyplex could be used as a potential RNA/DNA carrier for rapid endothelialization in vascular tissue engineering.

Acknowledgements

This work was supported by the Natural Science Foundation of China under Grant No. 51473118, No. 11372030 and No. 11421202.

References

1 A. Zampetaki and M. Mayr, *Circ. Res.*, 2012, **110**, 508–522.
2 Y. Suarez and W. C. Sessa, *Circ. Res.*, 2009, **104**, 442–454.
3 E. Allen, Z. Xie, A. M. Gustafson and J. C. Carrington, *Cell*, 2005, **1212**, 207–221.
4 M. Muthiah, I. Park and C. Cho, *Expert Opin. Drug Delivery*, 2013, **10**, 1259–1273.
5 E. N. James, A. M. Delany and L. S. Nair, *Acta Biomater.*, 2014, **10**, 3571–3580.
6 I. M. Castaño, C. M. Curtin, G. Shaw, J. M. Murphy, G. P. Duffy and F. J. O'Brien, *J. Controlled Release*, 2015, **200**, 20042–20051.
7 S. Wang, A. B. Aurora, B. A. Johnson, X. X. Qi, J. McAnally, J. A. Hill, J. A. Richardson, R. Bassel-Duby and E. N. Olson, *Dev. Cell*, 2008, **15**, 261–271.
8 J. E. Fish, M. M. Santoro, S. U. Morton, S. Yu, R. F. Yeh, J. D. Wythe, K. N. Ivey, B. G. Bruneau, D. Y. R. Stainier and D. Srivastava, *Dev. Cell*, 2008, **15**, 272–284.
9 R. Zhao, W. Hou, Z. Zhang, L. Qian and L. Jiang, *J. Nanosci. Nanotechnol.*, 2015, **15**, 2088–2093.
10 Z. Yang, Q. Tu, J. Wang and N. Huang, *Biomaterials*, 2012, **33**, 6615–6125.
11 J. Melchiorri, N. Hibino and J. P. Fisher, *Tissue Eng., Part B*, 2013, **19**, 292–307.
12 E. T. Goh, E. Wong, Y. Farhatnia, A. Tan and A. M. Seifalian, *Int. J. Mol. Sci.*, 2015, **16**, 597–627.
13 H. Kurobe, M. W. Max field, C. K. Breuer and T. Shinoka, *Stem Cells Transl. Med.*, 2012, **1**, 566–571.
14 Y. Wei, Y. Ji, L. Xiao, Q. Lin, J. Xu, K. Ren and J. Ji, *Biomaterials*, 2013, **34**, 2588–2599.
15 H. Ceylan, A. B. Tekinay and M. O. Guler, *Biomaterials*, 2011, **32**, 8797–8805.
16 J. A. Hubbell, S. P. Massia, N. P. Desai and P. D. Drumheller, *Nat. Biotechnol.*, 1991, **9**, 568–572.
17 C. Shi, Q. Li, W. Zhang, Y. Feng and X. Ren, *ACS Appl. Mater. Interfaces*, 2015, **7**, 20389–20399.
18 Y. Yang, S. Wang, Y. Wang, X. Wang, Q. Wang and M. Chen, *Biotechnol. Adv.*, 2014, **32**, 1301–1316.
19 S. Mao, W. Sun and T. Kissel, *Adv. Drug Delivery Rev.*, 2010, **62**, 12–27.
20 C. Jonker, J. H. Hamman and A. F. Kotze, *Int. J. Pharm.*, 2002, **238**, 205–213.
21 S. Mao, X. Shuai, F. Unger, M. Wittmar, X. L. Xie and T. Kissel, *Biomaterials*, 2005, **26**, 6343–6356.
22 O. Germershaus, S. Mao, J. Sitterberg, U. Bakowsky and T. Kissel, *J. Controlled Release*, 2008, **125**, 145–154.
23 Y. Gao, Z. Wang, J. Zhang, Y. Zhang, H. Huo, T. Wang, T. Jiang and S. Wang, *Biomacromolecules*, 2014, **15**, 1010–1018.
24 M. Miteva, K. C. Kirkbride, K. V. Kilchrist, T. A. Werfel, H. Li, C. E. Nelson, M. K. Gupta, T. D. Giorgio and C. L. Duvall, *Biomaterials*, 2015, **38**, 97–107.
25 X. Zhang, J. Yao, L. Zhang, J. Fang and F. Bian, *Carbohydr. Polym.*, 2014, **103**, 566–572.
26 H. Wang, Y. Feng, Y. Yang, J. Guo and W. Zhang, *J. Mater. Chem. B*, 2015, **3**, 3379–3391.
27 A. Polnok, G. Borchard, J. C. Verhoef, N. Sarisut and H. E. Junginger, *Eur. J. Pharm. Biopharm.*, 2004, **57**, 77–83.
28 D. Liu, X. Zhang, C. Yan, Y. Li, X. Tian, N. Zhu, J. Rong, C. Peng and Y. Han, *Thromb. Res.*, 2015, **135**, 146–154.
29 C. Fella, G. F. Walker, M. Ogris and E. Wagner, *Eur. J. Pharm. Sci.*, 2008, **34**, 309–320.
30 H. L. Jiang, Y. K. Kim, R. Arote, J. W. Nah, M. H. Cho, Y. J. Choi, T. Akaike and C. S. Cho, *J. Controlled Release*, 2007, **117**, 273–280.
31 H. Katas and H. Alpar, *J. Controlled Release*, 2006, **115**, 216–225.
32 S. Lelu, S. P. Strand, J. Steine and C. L. Davies, *Biomacromolecules*, 2011, **12**, 3656–3665.
33 S. Singh, A. S. Narang and R. I. Mahato, *Pharm. Res.*, 2011, **28**, 2996–3015.
34 N. James, A. M. Delany and L. S. Nair, *Acta Biomater.*, 2014, **10**, 3571–3580.
35 C. Zhang, B. Guo, H. Wu, T. Tang, B. Zhang, L. Zheng, Y. He, Z. Yang, X. Pan, H. Chow, K. To, Y. Li, D. Li, X. Wang, Y. Wang, K. Lee, Z. Hou, N. Dong, G. Li, K. Leung, L. Hung, F. He, L. Zhang and L. Qin, *Nat. Med.*, 2012, **18**, 307–314.